

Structure and Morphology of Electrodeposited Nickel Nanowires at an Electrode Distance of 20mm

Mahendran Samykano , Ram Mohan, Shyam Aravamudhan

Abstract—The objective of this work is to study the effect of two key factors - external magnetic field and applied current density during template-based electrodeposition of nickel nanowires using an electrode distance of 20 mm. Morphology, length, crystallite size and crystallographic characterization of the grown nickel nanowires at an electrode distance of 20mm are presented. For this electrode distance of 20 mm, these two key electrodeposition factors when coupled was found to reduce crystallite size with a higher growth length and preferred orientation of Ni crystals. These observed changes can be inferred to be due to coupled interaction forces induced by the intensity of applied electric field (current density) and external magnetic field known as magnetohydrodynamic (MHD) effect during the electrodeposition process.

Keywords—Anodic alumina oxide, electrodeposition, nanowires, nickel.

I. INTRODUCTION

MAGNETIC 1 dimensional nanostructures are interesting not only from their fundamental properties perspective but also for the range of applications that include high-density magnetic storage, sensors, planer microwave circuit and medicine. Nickel (Ni) is among four elements which has excellent ferromagnetic properties, along with good corrosion stability. Several methods and processing conditions have been developed to synthesize 1-D nanostructures of various sizes, morphology and composition that have resulted in exciting and fundamentally different configurations [1], [2].

1-D magnetic nanostructures can be produced by a number of techniques indulging vapor-liquid-solid growth [3], focused ion beam [4], sol-gel [5], nanolithography [6], molecular beam epitaxy [7] and electrodeposition [8]. Metal electrodeposition into channels of porous materials (such as anodic alumina membranes, track-etched polymer membranes, nanochannel glass, block copolymer and mesoporous silica) is one of the common and elegant methods to produce one-dimensional nanostructures [8]-[10].

In an electrodeposition process, crystallization of electrodeposited metal is influenced not only by the composition and concentration of the electrolyte but also by

the processing conditions such as current density, temperature, electrolyte pH and agitation [11]. Another factor in the process is also electrode distance and ensuring the repeatable, correct electrode distance. The effect of current density on the structure and quality of the electrodeposit is particularly significant as it principally changes the cathodic potential [12]. Application of an external magnetic field during electrodeposition can induce currents in a conductive fluid which in turn can create forces acting on the fluid. The primary influence of an external magnetic field is due to the Lorentz force that acts on the moving electrolyte ions. As suggested by [13] and later verified by [14], this force induces a convective flow of the electrolyte near the template surface. This effect known as the magnetohydrodynamic (MHD) effect in electrodeposition process [15], [16] causes a decrease in the thickness of the diffusion layer, increase in the mass-transport of active species (ions) [17]-[19]. Structural and morphology changes due to independent [14], [20] and coupled effects [22] at a larger electrode distance have been studied. Present paper reports our recent data based on an electrode distance of 20 mm while employing two electric field (current density) conditions, with and without an external magnetic field. The morphology, growth length, crystallographic orientation, and crystallite size of Ni nanowires embedded inside the nanochannels of anodic alumina oxide (AAO) membrane at an electrode distance of 20mm are presented.

II. EXPERIMENTAL DETAILS

A. Nickel Nanowire Synthesis

In our present work, 1-D Nickel nanowire arrays were prepared by electrodeposition of Ni ions into the pores of Anopore® alumina oxide (AAO) template with an average pore diameter of 200 nm (Whatman, Germany). Further details of the electrodeposition method followed are presented in [22]. Prior to the electrochemical deposition, a special holder was fabricated using 3D printing technology so as to enable precise control of the distance and alignment of electrode, template and magnetic field direction for the present 20 mm electrode distance. Fig. 1 (a) shows the image of the holder fabricated with a span distance of 20mm (electrode distance) used in the present study. This holder was placed in the electrochemical bath for electrodeposition as shown in Fig. 1 (b). Nanowire synthesis was performed either with or without magnetic field. For nanowire synthesis with magnetic field, known magnetic field intensity was placed close to the template and electrode (with magnetic field parallel to nanowire growth). All parameters such as the solution pH, agitation conditions, temperature, external magnetic field,

M. Samykano is with the Joint School of Nanoscience and Nanoengineering, North Carolina A&T State University, Greensboro, NC 27401 USA (phone: 336-285-2867; fax: 336-500-0115; e-mail: mahendran.samykano@gmail.com).

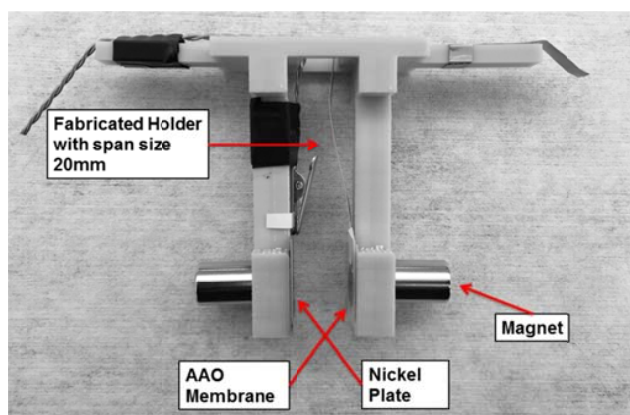
R.V. Mohan is with the Joint School of Nanoscience and Nanoengineering, North Carolina A&T State University, Greensboro, NC 27401 USA (e-mail: rvmohan@ncat.edu).

S. Aravamudhan is with the Joint School of Nanoscience and Nanoengineering, North Carolina A&T State University, Greensboro, NC 27401 USA (e-mail: saramu@ncat.edu).

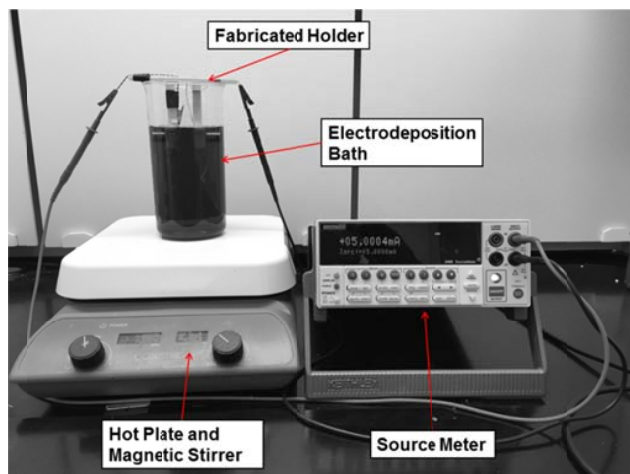
solution additives and deposition time, etc., were maintained to be consistent during the electrodeposition process except for the external magnetic field and current density for this electrode distance of 20 mm. Table I lists the two values of the current density and magnetic field used in the present work. All synthesis was done for 1 hour at a temperature of 35°C. After the electrodeposition process, the templates were cleaned with deionized water prior to dissolution in Sodium Hydroxide (NaOH) solution to obtain freestanding Nickel nanowires. Subsequently, NaOH solution was replaced with methanol solution.

TABLE I
DEPOSITION PROCESS PARAMETERS DURING SYNTHESIS

Parameter	Value	Units
Magnetic Field	0 and 5758	Gauss
Current Density	3 and 7	mA.cm^{-2}



(a)



(b)

Fig. 1 (a) 3D Printed Sample Holder, (b) Electrodeposition Set-up for Ni Nanowire Synthesis

B. Energy Dispersive Spectroscopy (EDS) and Scanning Electron Microscopy (SEM)

The free standing Ni nanowires in methanol solution were

dispersed on a Silicon substrate for elemental analysis with EDS performed at beam source of 15 kV. The same samples were analyzed for structure, morphology, including growth length and nanowire diameter in an SEM (Auriga, Carl Zeiss), using a beam source of 5 kV and 20 μm aperture size.

C. X-Ray Diffraction (XRD)

Free standing Ni nanowires in methanol solution were dispersed on a microscopic glass slide and later transferred into XRD capillary tube for diffraction experiments. X-ray diffraction were performed using a Gemini XRD (Keysight Technologies) with a monochromatized $\text{Cu K}\alpha$ ($\lambda = 0.154 \text{ nm}$) radiation source operated at 40 kV and 40 mA in a powder diffraction arrangement.

III. RESULTS AND DISCUSSION

A. EDS and SEM

The synthesized nanowires with an electrode distance of 20 mm for the two current densities studied, with and without the magnetic field were found to have an average diameter of $245 \pm 36 \text{ nm}$.

The elemental composition of the Ni nanowires deposited in the AAO template at different synthesis conditions obtained using EDS analysis indicated a composition of $98.27 \pm 0.4\%$ of Ni and $1.73 \pm 0.4\%$ of oxygen. The small amount of oxygen observed is primarily due to absorption from the air on the surface of the nanowires.

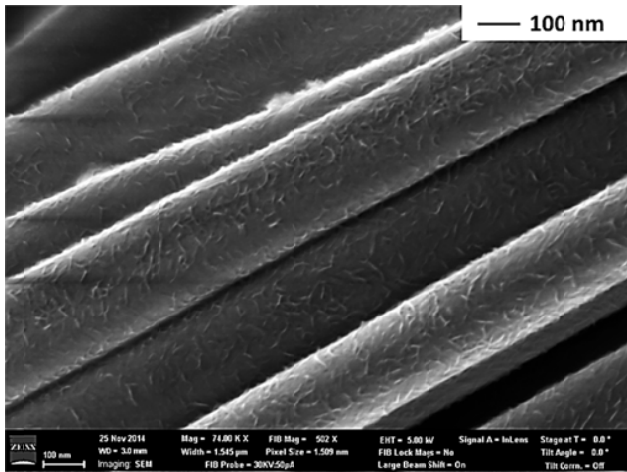
Figs. 2 and 3 shows the SEM image of surface morphology of the grown Ni nanowires at two current densities and magnetic fields studied. Fig. 2 shows the SEM image of surface morphology of Ni nanowires electrodeposited at current density of 3 mA.cm^{-2} and magnetic field of 0 G and 5758 G respectively. Fig. 3 shows the SEM images of surface morphology of Ni nanowire electrodeposited at 7 mA.cm^{-2} and magnetic field of 0 G and 5758 G respectively. SEM images indicate that the surface texture and roughness to be drastically reduced as the magnetic field strength is increased. These correlate well with findings observed by [21] on electrodeposited Ni thin films with applied magnetic field and in our previous work findings with an electrode distance larger than 20mm [22].

Next, the growth length of Ni nanowires at all synthesis conditions was measured to determine the influence of coupled magnetic field and current density on the growth rate of nanowires.

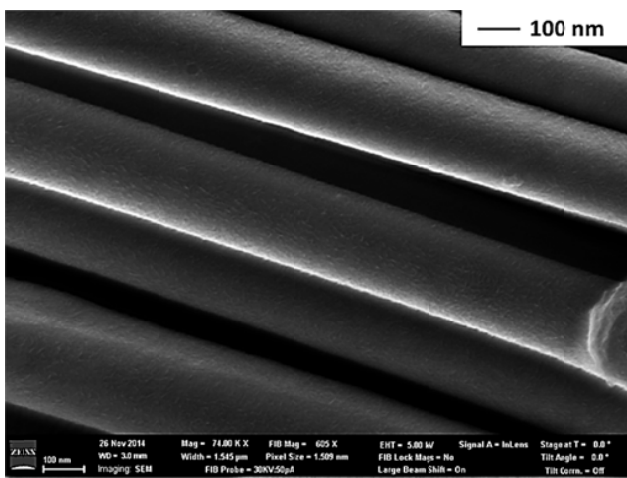
Fig. 4 presents the measured wire length distribution for the different process condition parameters. The growth rate is found to be significantly higher when the current density is increased. The growth rate is also found to show an increase with the magnetic field for the same current density.

B. X-Ray Diffraction Analysis (XRD)

XRD analysis based on powder diffraction method as presented in Figs. 5 and 6 shows the presence of multiple XRD peaks, which suggests that the grown Ni nanowires are polycrystalline in nature.



(a)



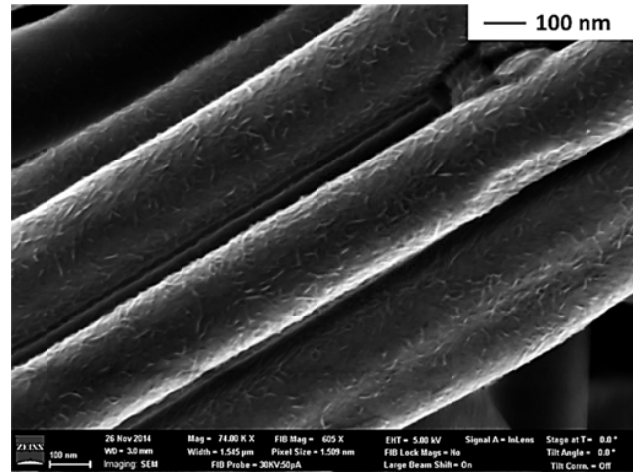
(b)

Fig. 2 SEM surface texture images grown at current density $3 \text{ mA}\cdot\text{cm}^{-2}$ and external magnetic field of, (a) 0G and (b) 5758G

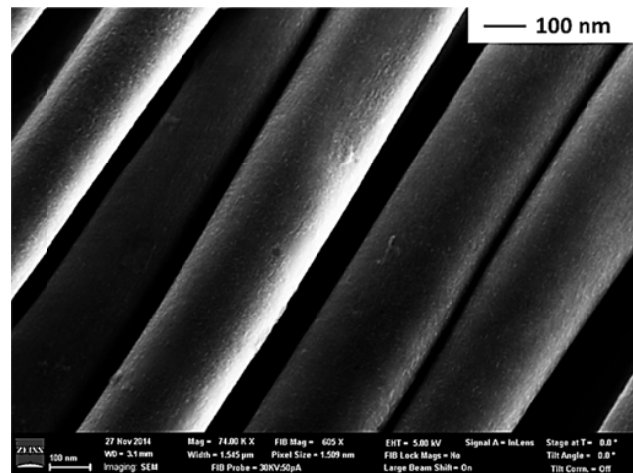
Fig. 5 shows that significant differences in the superimposed XRD spectra obtained for Ni electrodeposition at an electrode distance of 20 mm, current density of $3 \text{ mA}\cdot\text{cm}^{-2}$ at different magnetic fields – 0 G (solid line) and 5758G (dashed line). In the absence of magnetic field during synthesis, a strong peak of (1 1 1) Ni plane with other lower peaks of (2 0 0), (2 2 0), (3 1 1) and (2 2 2) Ni was observed. With external magnetic field, the (1 1 1) Ni peaks are significantly different and (2 0 0) Ni peaks change slightly, while others remain unchanged. In the presence of magnetic field during processing at this 20 mm electrode distance, Ni crystals is found to preferentially orient at (1 1 1) plane since the (1 1 1) plane is the easy magnetization plane for Ni magnetic structures.

Fig. 6 presents the superimposed XRD spectra obtained at a higher current density of $7 \text{ mA}\cdot\text{cm}^{-2}$ and at different external magnetic fields – 0 G (solid line) and 5756 G (dashed line). In the absence of external magnetic field, a strong peak of (1 1 1) Ni plane with other lower peaks of (2 0 0), (2 2 0), (3 1 1) and

(2 2 2) was observed. On application of magnetic field, the peaks were found not to show a significant change. This suggests the higher current density strength in this case ($7 \text{ mA}\cdot\text{cm}^{-2}$) has a stronger influence on the orientation, with little effect from the presence of magnetic field.



(a)



(b)

Fig. 3 SEM surface texture images grown at current density $7 \text{ mA}\cdot\text{cm}^{-2}$ and external magnetic field of, (a) 0G and (b) 5758G

Braggs formulation and Scherrer equation were used to quantitatively determine the crystallite sizes. Fig. 7 shows the average crystallite sizes obtained. The results clearly show a reduction in crystallite size with the presence of external magnetic field for both current densities studied for an electrode distance of 20 mm.

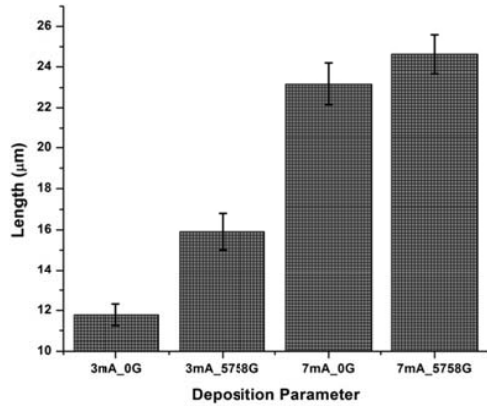


Fig. 4 Ni nanowire grown length at different proses condition (error bars: standard deviation, n=10)

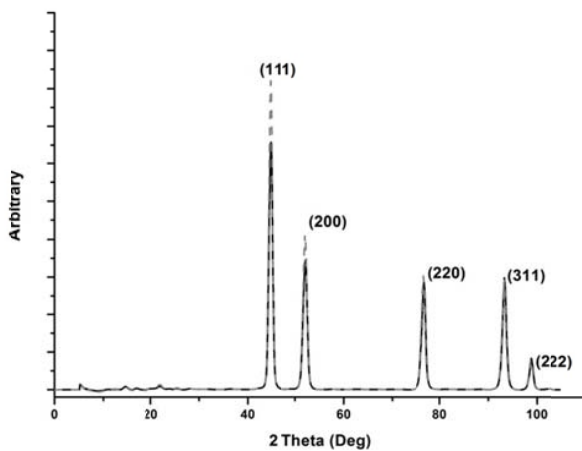


Fig. 5 X-ray diffraction spectra of the Ni nanowires deposited in alumina membranes at current density of 3 mA.cm^{-2} , and magnetic fields of 0G (solid line) and 5758G (dashed line)

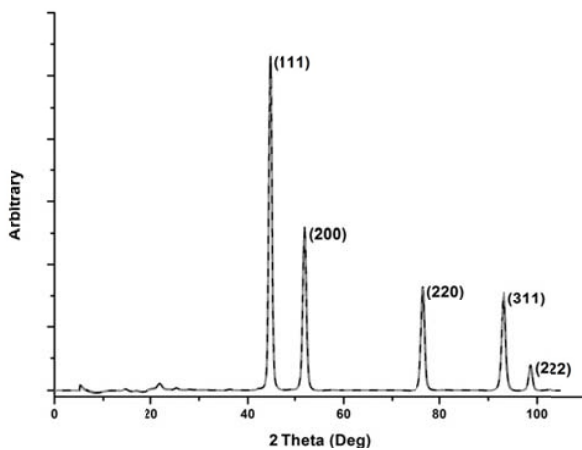


Fig. 6 X-ray diffraction spectra of the Ni nanowires deposited in alumina membranes at current density of 3 mA.cm^{-2} , and magnetic fields of 0G (solid line) and 5758G (dashed line)

This reduction in crystal size with the presence of magnetic field at both the current densities studied for an electrode distance of 20 mm could be due to enhanced nucleation of

active species during the electrodeposition process caused by the coupled effect of increased current density and applied magnetic field. The application of magnetic field enhances the convective flow and its ionic mass transport near the template during electrodeposition process, which also affects the deposition rate and reduces the diffusion controlling process. The diffusion processes tends to control grain growth, and a different model of grain growth as seen with the change in crystal size can be expected when a magnetic field is imposed during electrodeposition [23].

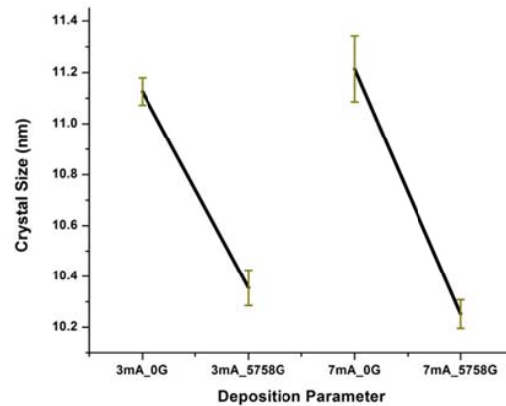


Fig. 7 Crystal size of deposited Ni nanowires at different process condition (error bars: standard deviation, n=5)

IV. CONCLUSION

Present paper reported the morphological, growth length, crystallographic properties and crystallite size of the Ni nanowires obtained during electrodeposition process at an electrode distance of 20mm studied using two electric field conditions with and without the presence of a magnetic field conditions. The presence of magnetic field at both current densities influenced the surface texture roughness, crystal orientation; overall growth length and crystallite size of the electrodeposited Ni nanowires. Surface texture of the nanowires was found to improve with the application of the magnetic field. Present study indicates that crystallographic orientation differences to be more predominant at lower current density compared to that at a higher current density when added magnetic field is employed. The crystal sizes were observed to reduce by nearly 11% due to application of magnetic field. Overall, the growth length was found to improve with an increase in the current density and magnetic field during processing for the electrode distance of 20 mm. All the changes seen could be due to coupled interaction forces induced by intensity of applied electric field (current density) and magnetic field known as magnetohydrodynamic (MHD) effect during the electrodeposition process.

ACKNOWLEDGMENT

This work was supported by Joint School of Nanoscience and Nanoengineering (JSNN), North Carolina A&T State University and Universiti Malaysia Pahang, Ministry of Education, Malaysia.

REFERENCES

- [1] J. Chen, B. J. Wiley, and Y. Xia, "One-dimensional nanostructures of metals: large-scale synthesis and some potential applications," *Langmuir* 23, No. 8, 2007, pp. 4120-4129.
- [2] Y. Xia, P. Yang, Y. Sun, Y. Wu, B. Mayers, B. Gates, Y. Yin, F. Kim, and H. Yan, "One-dimensional nanostructures: synthesis, characterization, and applications," *Advanced Materials* 15, No. 5, 2003, pp. 353-389.
- [3] C. A. Decker, R. Solanki, J. L. Freeouf, J. R. Carruthers, and D. R. Evans, "Directed growth of nickel silicide nanowires," *Applied physics letters* 84, No. 8, 2004, pp. 1389-1391.
- [4] S. E. Wu, Y. W. Huang, T. H. Hsueh, and C. P. Liu, "Fabrication of nanopillars comprised of InGaN/GaN multiple quantum wells by focused ion beam milling," *Japanese Journal of Applied Physics* 47, No. 6S, 2008, p. 4906.
- [5] X. Wang, X. Wang, W. Huang, P. J. Sebastian, and S. Gamboa, "Sol-gel template synthesis of highly ordered MnO₂ nanowire arrays," *Journal of Power Sources* 140, No. 1, 2005, pp. 211-215.
- [6] W. Li, M. W. Qiu, M. Hu, Z. C. Liu, Z. L. Zhao, Z. Tao, D. Y. Chen, and Y. Jiang, "Sub-100 nm Single Crystalline Periodic Nano Silicon Wire Obtained by Modified Nanoimprint Lithography," *Nanoscience and Nanotechnology Letters* 5, No. 7, 2013, pp. 737-740.
- [7] S. Chikazumi, "Epitaxial Growth and Magnetic Properties of Single-Crystal Films of Iron, Nickel, and Permalloy," *Journal of Applied Physics* 32, No. 3, 1961, pp. S81-S82.
- [8] Huczko, A., "Template-based synthesis of nanomaterials," *Applied Physics A* 70, No. 4, 2000, pp. 365-376.
- [9] C. R. Martin, "Membrane-based synthesis of nanomaterials," *Chemistry of Materials* 8, No. 8, 1996, pp. 1739-1746.
- [10] J. C. Hulteen, "A general template-based method for the preparation of nanomaterials," *Journal of Materials Chemistry* 7, No. 7, 1997, pp. 1075-1087.
- [11] A. Cortés, G. Riveros, J. L. Palma, J. C. Denardin, R. E. Marotti, E. A. Dalchiale, and H. Gómez, "Single-crystal growth of nickel nanowires: influence of deposition conditions on structural and magnetic properties," *Journal of nanoscience and nanotechnology* 9, No. 3, 2009, pp. 1992-2000.
- [12] C. H. Siah, N. Aziz, Z. Samad, M. N. Idris, and M. A. Miskam, "A Review of the Fundamental Studies for the Electroplating Process," 2002, Universiti Sains Malaysia, unpublished.
- [13] I. Tabakovic, S. Riemer, V. Vas'ko, V. Sapozhnikov, and M. Kief, "Effect of magnetic field on electrode reactions and properties of electrodeposited NiFe films," *Journal of The Electrochemical Society* 150, No. 9, 2003, pp. C635-C640.
- [14] S. Aravamudhan, J. Singleton, P. A. Goddard, and S. Bhansali, "Magnetic properties of Ni-Fe nanowire arrays: effect of template material and deposition conditions," *Journal of Physics D: Applied Physics* 42, No. 11, 2009, p. 115008.
- [15] O. Devos, A. Olivier, J. P. Chopart, O. Aaboubi, and G. Maurin, "Magnetic field effects on nickel electrodeposition," *Journal of The Electrochemical Society* 145, No. 2, 1998, pp. 401-405.
- [16] A. Ispas, H. Matsushima, W. Plieth, and A. Bund, "Influence of a magnetic field on the electrodeposition of nickel-iron alloys," *Electrochimica acta* 52, No. 8, 2007, pp. 2785-2795.
- [17] G. Hinds, J. M. D. Coey, and M. E. G. Lyons, "Influence of magnetic forces on electrochemical mass transport," *Electrochemistry communications* 3, No. 5, 2001, pp. 215-218.
- [18] A. Bund, S. Koehler, H. H. Kuehnlein, and W. Plieth, "Magnetic field effects in electrochemical reactions," *Electrochimica Acta* 49, No. 1, 2003, pp. 147-152.
- [19] H. Matsushima, A. Ispas, A. Bund, and B. Bozzini, "Magnetic field effects on the initial stages of electrodeposition processes," *Journal of Electroanalytical Chemistry* 615, No. 2, 2008, pp. 191-196.
- [20] C. Gong, L. Yu, Y. Duan, J. Tian, Z. Wu, and Z. Zhang, "The fabrication and magnetic properties of Ni fibers synthesized under external magnetic fields," *European Journal of Inorganic Chemistry*, No. 18, 2008, pp. 2884-2891.
- [21] J. Rabia, H. Tajamal, S. Saliha, and A. M. Shahid, "Magnetic Field Effects on the Microstructural Variation of Electrodeposited Nickel Film," *Journal of Materials Science and Engineering A: Structural Materials: Properties, Microstructure and Processing* 1, No. 4, 2011, pp. 481-487.
- [22] Samykano, M., Mohan, R., and Aravamudhan, S., "Morphology and Crystallographic Characterization of Nickel Nanowires—Influence of Magnetic Field and Current Density During Synthesis," *Journal of Nanotechnology in Engineering and Medicine*, 5(2), 2014, p. 021005.
- [23] H. R. Khan, and K. Petrikowski, "Magnetic field effects on electrodeposition of cobalt film and nanowires," *In Materials Science Forum*, Vol. 373, 2001, pp. 725-728.